Journal of Atomic and Molecular Sciences

ISSN 2075-1303

Global Science Press

Influences of the low collision energies and isotopic variants on the stereodynamics for reactions Li+DF/TF→LiF+D/T

Received Oct. 13, 2017,
Accepted Dec. 12, 2017,

DOI: 10.4208/jams.101317.121217a

http://www.global-sci.org/jams/

Xin Zhuang[a], Junmei Song[a], Luyan Sun[a], Tiantian Wang[a] and Xinguo Liu[a *]

Abstract. Stereodynamics for Li+DF/TF→LiF+D/T reactions are studied using the quasi-classical trajectory method based on a new potential energy surface constructed by Aguado and Paniaga [J. Chem. Phys. 119 (2003) 10088]. The product angular distributions of $P(\theta_r)$ and $P(\phi_r)$, which reflect the vector correlation, are calculated and discussed. The average rotational alignment factor $\langle P_2(\cos\theta_r)\rangle$ as function of the collision energy is also presented. Furthermore, four polarization-dependent differential cross sections (PDDCSs), namely, $PDDCS_{00}$, $PDDCS_{20}$, $PDDCS_{21-}$ and $PDDCS_{22+}$ are calculated as well. By comparing the stereodynamics results of the title reactions, we find that the isotopic effects are relatively obvious.

Keywords: Quasi-classical trajectory; Stereodynamics; Product angular distribution; Polarization-dependent generalized differential cross sections; Mass factor

1. Introduction

The Li+HF→LiF+H reaction, which serves as a prototype for textbook reactions between alkali metals and hydrogen halides, has attracted a lot of attentions from both experimental[1-5] and theoretical[6-16] aspects. The first crossed molecular beam experiment on the LiFH system was carried out by Becker *et al.* in 1980 to detect the product angular distribution.[1] Subsequently, the Li+HF(*v*=1,*j*=1,m=0)→LiF+H reaction was studied in detail by Loesch *et al*. at the collision energy of 420 meV.[2-4] Using crossed molecular beam apparatus, Höbel *et al*. measured the double differential cross sections for the Li+HF→LiF+H reaction at collision energies ranging from 88 to 378 meV.[5]

In terms of theory, the Li+HF→LiF+H reaction, with few electrons, is relative simple, which provides likelihood to perform high-quality *ab initio* calculations for constructing an ideal potential energy surface (PES). There is a relatively deep van der Waals well in the reagent valley and a strongly bent transition state with a considerable barrier in the exit channel,[17] which makes the title reaction system possessing abundant dynamic information. In 1995, Aguado *et al*. constructed the PES of the reaction using the multiple reference single and double excitations configureuration-interaction (MRDCI) method.[18] Soon afterwards, the same group presented a new fit to the more accurate MRDCI *ab initio* PES.[14] Moreover, they carried out the quantum dynamics study based on local coordinates using a three-dimensional time-dependent method, which makes it possible to describe reactants and products at the same time. In 2003, Aguado *et al*. performed high level *ab initio* calculations for a large number of nuclear configurations (about 6000) based on a new atomic basis sets and fitted four analytic global PESs for three $^2A'$ and one $^2A''$ electronic states. [17] Furthermore, they simulated spectrum of the LiHF system with the new PES, which is in very good agreement with the experimental data of Hudson et al.[19]

Lagana *et al.* presented zero total angular momentum exact quantum probabilities for Li+HF and its isotopic variants reactions in 2000.[20] Wecka *et al*. carried out a quantum reactive scattering calculations for zero total angular momentum at low and ultralow temperatures in 2005.[8] Based on the AP2-PES(1997), Yuan and Zhao explored the scalar and vector properties using the quasi-classical trajectory (QCT) method, aiming at studying the stereodynamics features of the reaction system in 2010.[21] Recently, based on the ground state PES, Liu *et al.* studied the vector properties of the Li+HF→LiF+H as well as its isotopic variant reactions at translational collision energies ranging from 30 kcal/mol to 60 kcal/mol using the QCT method.[22] Soon afterwards, the same group investigated the stereodynamics properties for the same reaction at collision energies ranging from 1.15 kcal/mol to 5.0 kcal/mol.[23] However, except the research carried out by Liu *et al.,* [22, 23] it is rare to study the LiHF system based on the new PES. Nevertheless, the Liu's group didn't investigate the isotopic substitution of the system when the collision energy is not more than 5.0 kcal/mol. In order to fully characterize stereodynamics of the isotopic substitution of Li+HF reaction at lower collision energy, we explore the vector properties for Li+DF/TF→LiF+D/T reactions using the QCT method based on the new PES constructed by Aguado et al. over a collision energy range of 2.5-5.0 kcal/mol.

2. Theory

In this work, the adopted accurate full dimensional PES constructed by Aguado et al.[17] which takes the following form written as,

$$V_{ABC} = \sum_A V_A^{(1)} + \sum_{AB} V_{AB}^{(2)}(R_{AB}) + V_{ABC}^{(3)}(R_{AB}, R_{AC}, R_{BC})$$

Where $\boldsymbol{V_A^{(1)}}$ is the energy of atom A in its appropriate electronic state, and the value of $\sum_A \boldsymbol{V_A^{(1)}}$ is usually taken as zero because all the atoms are in their ground state. Moreover, $\boldsymbol{V_{AB}^{(2)}}$ and $\boldsymbol{V_{ABC}^{(3)}}$ are the two-body and three-body energy term respectively. In addition, $\boldsymbol{R_{AB}}$, $\boldsymbol{R_{AC}}$, and $\boldsymbol{R_{BC}}$ represent the distances of *AB*, *AC*, *BC* respectively.

[a] School of Physics and Electronics, Shandong Normal University, Jinan 250014. China
* Corresponding author. Email address: liuxinguo@sdnu.edu.cn

Based on the new PES, we carried out the dynamical calculations by employing the stereo-QCT procedure developed by Han et al.[24-31] The classical Hamilton equations are numerically integrated in three dimensions. In order to ensure the conservation of total energy and angular momentum, the integration step size is chosen to be 0.1 fs. The impact parameter *b* is optimized through the repeated computations with 100000 trajectories. The maximum impact parameter $\boldsymbol{b_{max}}$ is obtained where there is no reactive trajectory anymore when the value of b is slightly increased. The present QCT calculations are performed in the center-of-mass (CM) frame, depicted in Figure 2.1.

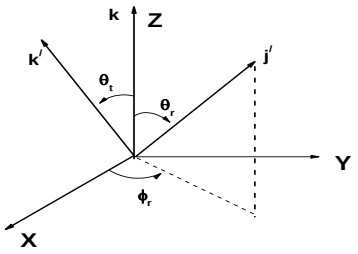

Figure 2.1: Centre-of-mass coordinate system used to describe the ***k***, ***k'*** and ***j'*** correlations.

3. Results and discussion

Figure 3.1 displays the product angular distributions of $\boldsymbol{P(\theta_r)}$ representing $\boldsymbol{k-j'}$ correlation at different collision energies. As can be seen in Figure 3.1 (a), all $\boldsymbol{P(\theta_r)}$ distributions of Li+DF→LiF+D reaction at different collision energies from 2.5 kcal/mol to 5.0 kcal/mol show a prominent peak at $\boldsymbol{\theta_r = 90^\circ}$ and are symmetric with respect to $\boldsymbol{\theta_r = 90^\circ}$, which means that the product rotational angular momentum vector $\boldsymbol{j'}$ is perpendicular to the direction of the reagent relative velocity $\boldsymbol{k}$ and indicates that the $\boldsymbol{P(\theta_r)}$ distribution has a strong product rotational alignment. Furthermore, there is an obvious trend that the peaks of the product $\boldsymbol{P(\theta_r)}$ distribution become higher with the increase of the collision energy from 2.5 kcal/mol to 5.0 kcal/mol, which shows that the product alignment becomes stronger as the collision energy increases. In addition, in Figure 3.1 (b), there exist almost the same phenomena except a little bit discrepancy for the isotopic reaction Li+TF→LiF+T at different collision energies from 2.5 kcal/mol to 5.0 kcal/mol. The value of $\boldsymbol{P(\theta_r)}$ at $\boldsymbol{\theta_r = 90^\circ}$ becomes higher with the collision energies change from 2.5 kcal/mol to 4.0 kcal/mol and the highest appears at 4.0 kcal/mol while the value becomes lower with the collision energies changing from 4.0 kcal/mol to 5.0 kcal/mol, which means the change of the product alignment is not a monotonic enhancement with increasing collision energies for Li+TF→LiF+T reaction. Moreover, there is a prominent feature observed in Figure 3.1 (a) and (b) that the $\boldsymbol{P(\theta_r)}$ value of the Li+DF→LiF+D reaction at $\boldsymbol{\theta_r = 90^\circ}$ is larger than that of the Li+TF→LiF+T reaction at the same collision energy, which means that the product alignment of the Li+DF→LiF+D reaction is stronger than the Li+TF→LiF+T reaction. As discussed in Refs [27, 29] the $\boldsymbol{P(\theta_r)}$is sensitive to two factors: one is the character of the PES and the other is the mass factor $\boldsymbol{\cos^2\beta}$ (i.e. $\boldsymbol{\cos^2\beta = m_A m_C/(m_A+m_B)(m_B+m_C)}$ for the A+BC→AB+C reaction. For reactions Li+ DF/TF→LiF+D/T, the mass factor $\boldsymbol{\cos^2\beta}$ is 0.02585 and 0.03695 respectively. Since the same PES is adopted in the calculation, the change of the $\boldsymbol{P(\theta_r)}$distributions is due to the difference in mass factor of the reactions, that is, the $\boldsymbol{P(\theta_r)}$ distributions are affected by isotope effect. The product rotational angular momentum is approximately equal to the reactant orbital angular momentum, and the reactant orbital angular momentum plays an important role on the distribution of $\boldsymbol{P(\theta_r)}$ for HHL mass combination. [29]Therefore, large mass factor of the reactions will have larger product rotational angular momentum, leading to the fact that the product rotational angular momentum alignment effect weakens with the mass factor increases. The dihedral angle of $\boldsymbol{P(\phi_r)}$ distributions, which describes the $\boldsymbol{k-k'-j'}$ correlation, shown in Figure 3.1 (c) and (d), can provide both product alignment and orientation information. From Figure 3.1 (c) and (d), it is clear that $\boldsymbol{P(\phi_r)}$ tends to be asymmetric with respect to the scattering plane, reflecting the strong polarization of angular momentum for Li+DF→LiF+D and Li+TF→LiF+T reactions at different collision energies. At the same time, the peaks of the product $\boldsymbol{P(\phi_r)}$ distributions of Li+DF→LiF+D reaction at $\boldsymbol{\phi_r = 270^\circ}$ become higher with the collision energy increase from 2.5 kcal/mol to 5.0 kcal/mol. However, for Li+TF→LiF+T reaction, while the value of the $\boldsymbol{P(\phi_r)}$ distribution at $\boldsymbol{\phi_r = 270^\circ}$becomes higher when the collision energies change from 2.5 kcal/mol to 4.5 kcal/mol, the peak of $\boldsymbol{P(\phi_r)}$ distribution at $\boldsymbol{\phi_r = 270^\circ}$ at 5.0 kcal/mol is lower than that of 4.5 kcal/mol, which means the peaks of the $\boldsymbol{P(\phi_r)}$ distributions for Li+TF→LiF+T reaction are not monotonic enhancement over the collision energies range of 2.5 kcal/mol to 5.0 kcal/mol. Furthermore, the values of all reactions at $\boldsymbol{\phi_r = 270^\circ}$ are much larger than at $\boldsymbol{\phi_r = 90^\circ}$, which reflects that the product rotational angular momentum is oriented along the negative y-axis and the product has a preference for left-handed rotation in planes which are parallel to the scattering plane. Generally speaking, as the collision energy increases, the values of the product $\boldsymbol{P(\phi_r)}$ distribution of Li+ DF/TF→LiF+D/T reactions become higher. Similar to $\boldsymbol{P(\theta_r}$ distributions, the peaks of $\boldsymbol{P(\phi_r)}$ distributions for Li+DF→LiF+D reaction are larger than that for Li+TF→LiF+T reaction at the same collision energy, which indicates that the degree of product orientation of the Li+DF→LiF+D reaction is stronger than that of Li+TF→LiF+T reaction. In this case, as discussed in Refs.[32, 33] we can deduce that the discrepancy of the orientation degree for the reaction may due to the different effective potential well depth of the reaction induced by the different harmonic zero point energy (ZPE) of the reactant molecules DF/TF. In the light of $\boldsymbol{\nu = \sqrt{k/\mu}/2\pi}$ and $\boldsymbol{E_0 = h\nu/2}$, the vibrational frequency of DF is higher than that of TF. Consequently, the depth of effective potential well for the Li+DF→LiF+D reaction is shallower than that of Li+TF→LiF+T reaction, which makes the degree of product orientation for the Li+DF→LiF+D reaction stronger. Such phenomenon can also be well explained qualitatively by the impulse model for the A+BC→AB+C reaction.[33-35] According to Refs.[33-35] we have $\boldsymbol{j' = Lsin^2\beta + jcos^2\beta + J_1 m_B/m_{AB}}$, where *L* is the reagent orbital angular momentum and $\boldsymbol{J_1 = \sqrt{\mu_{BC}R}(r_{AB}+r_{CB})}$, with $\boldsymbol{r_{AB}}$ and $\boldsymbol{r_{CB}}$ being the unit vectors for *B* pointing to *A* and *C*, respectively, $\boldsymbol{\mu_{BC}}$ is the reduced mass of the *BC* molecule and *R* is the repulsive energy between *B* and *C* atoms. Moreover, $\boldsymbol{cos^2\beta}$ is mass factor. During the whole reactive process for the Li+ DF/TF→LiF+ D/T reactions, since the term $\boldsymbol{Lsin^2\beta + jcos^2\beta}$ is symmetric, the term

$\boldsymbol{J_1 m_B/m_{AB}}$ will lead to the asymmetric of the $\boldsymbol{P(\phi_r)}$ distributions showing a preferred direction caused by the effect of the repulsive energy.

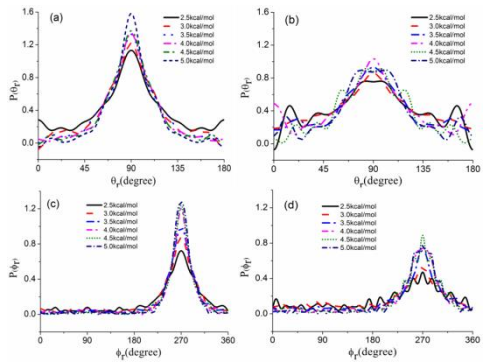

Figure 3.1: The distributions of $\boldsymbol{P(\theta_r)}$ for reactions (a) Li+DF→LiF+D, (b) Li+TF→LiF+T and the dihedral angle distribution of $\boldsymbol{P(\phi_r)}$ for (c) Li+DF→LiF+D, (d) Li+TF→LiF+T reactions at collision energies from 2.5 kcal/mol to 5.0 kcal/mol.

The degree of product rotational polarization of $\boldsymbol{j'}$ can also be described by the average rotational alignment factor $\langle \boldsymbol{P_2(\cos\theta_r)} \rangle$. The product rotational alignment parameters $\langle \boldsymbol{P_2(\cos\theta_r)} \rangle$ for Li+DF→LiF+D and Li+TF→LiF+T reactions at different collision energies have also been calculated in the present work, as displayed in the Figure 3.2. According to formula of $\langle \boldsymbol{P_2(\cos\theta_r)} \rangle$, the product rotational polarization is the strongest when the expected valuation $\langle \boldsymbol{P_2(\cos\theta_r)} \rangle$ is very close to -0.5. From Figure 3.2, we can find that the value of $\langle \boldsymbol{P_2(\cos\theta_r)} \rangle$ gets more close to -0.5 for Li+DF→LiF+D and Li+TF→LiF+T reactions with the increase of collision energy, which indicates the degree of product alignment becomes stronger. However, the value of $\langle \boldsymbol{P_2(\cos\theta_r)} \rangle$ for Li+DF→LiF+D reaction is less than that for Li+TF→LiF+T reaction at the same collision energy, which shows the product alignment of the Li+DF→LiF+D reaction is stronger than that of Li+TF→LiF+T reaction. These results are in good agreement with the $\boldsymbol{P(\theta_r)}$ distributions.

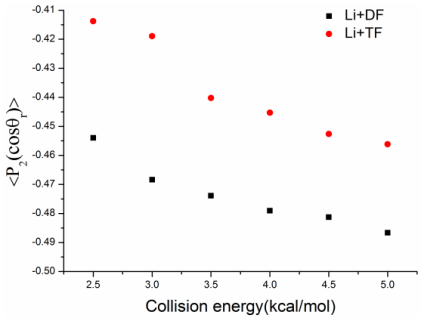

Figure 3.2: Variation of rotational alignment parameters $\langle \boldsymbol{P_2(\cos\theta_r)} \rangle$ for Li+DF/TF→LiF+D/T reactions at different collision energies.

Figure 3.3 shows the PDDCSs, that is, $\boldsymbol{(2\pi/\sigma)(d\sigma_{00}/dw_t)}$, $\boldsymbol{(2\pi/\sigma)(d\sigma_{20}/dw_t)}$, $\boldsymbol{(2\pi/\sigma)(d\sigma_{21-}/dw_t)}$ and $\boldsymbol{(2\pi/\sigma)(d\sigma_{22+}/dw_t)}$, describing the $\mathbf{k-k'-j'}$ correlation and the scattering direction of the product molecule. The $PDDCS_{00}$ and $PDDCS_{20}$ are displayed in Figure 3.3 (a) and (c) for the Li+DF→LiF+D and Li+TF→LiF+T reactions respectively. As a simple differential cross section, $PDDCS_{00}$ only describes the product angular distributions while it is not associated with the orientation or the alignment of the product rotational angular momentum vector. It is clearly seen that $PDDCS_{00}$ distributions for Li+DF→LiF+D and Li+TF→LiF+T reactions, shown in the upper half of Figure 3.3 (a) and (c), demonstrate both forward and backward scattering. However, different collision energies have different effects on the degree of forward scattering and backward scattering. Generally speaking, for reaction Li+DF→LiF+D, with the increase of the collision energy, the intensity of forward scattering becomes weaker while the degree of backward scattering stronger. On the contrary, for reaction Li+TF→LiF+T, as the collision energy increases, the degree of forward scattering becomes stronger while the intensity of backward scattering weaker. As is known, there is a well in the entrance channel on the PES of the title reactions so that the reactants are easily able to cross the well with the increase of collision energy. According to the law of conservation of energy, the product relative velocity vector of Li+TF→LiF+T reaction is less than that of Li+DF→LiF+D reaction at the same collision energy, leading to the fact that the product of the Li+DF→LiF+D reaction prefers to backward scattering while that of the Li+TF→LiF+T reaction prefers to forward scattering. Presented in the lower half of Figure 3.3 (a) and (c), $PDDCS_{20}$ distributions demonstrate an opposite trend to that of $PDDCS_{00}$, which may result from the fact that $PDDCS_{20}$ is related to alignment parameter $\langle \boldsymbol{P_2(\cos\theta_r)} \rangle$. As a whole, the expectation value of $PDDCS_{20}$ for Li+TF→LiF+T reaction is larger than that of Li+DF→LiF+D reaction. Thus, the degree of rotational alignment for Li+DF→LiF+D reaction is stronger than that of Li+TF→LiF+T reaction, which is in good agreement with the $\boldsymbol{P(\theta_r)}$and $\langle \boldsymbol{P_2(\cos\theta_r)} \rangle$ distributions. The $PDDCS_{21-}$ and $PDDCS_{22+}$ with $\boldsymbol{q \neq 0}$ are depicted in Figure 3.3 (b) and (d) for Li+DF→LiF+D and Li+TF→LiF+T reactions respectively. It is easy to find that all of the PDDCSs with $\boldsymbol{q \neq 0}$ are equal to zero at the extremities of forward and backward scatterings, resulting from that the $\boldsymbol{k-k'}$ scattering plane is not determined and the values of PDDCSs with $\boldsymbol{q \neq 0}$ must be zero at these limits of scattering angle. The PDDCSs with $\boldsymbol{q \neq 0}$, with scattering angles being $\boldsymbol{0 < \theta_t < 180^\circ}$, can provide detailed information about the product rotational alignment and orientation. The $PDDCS_{21-}$ is related to $\langle \boldsymbol{-\sin 2\theta_r \cos\phi_r} \rangle$ and the positive value of it corresponds to the product rotational angular momentum *j'* along the direction of Vector $\mathbf{x-z}$, while the negative value corresponds to *j'* along the direction of vector $\mathbf{x+z}$. As shown in Figure 3.3s (b) and (d), $PDDCS_{21-}$ values vary with the scattering angle changing, which implies that the product angular momentum distribution are anisotropic for Li+DF→LiF+D and Li+TF→LiF+T reactions. What's more, $PDDCS_{21-}$ distributions indicate the largest negative peaks at $\boldsymbol{\theta_t = 20^\circ}$ for both Li+DF→LiF+D and Li+TF→LiF+T reactions. At the same time, there are prominent large positive peaks around $\boldsymbol{53^\circ < \theta_t < 105^\circ}$ for Li+DF→LiF+D reaction. While there are prominent large positive peaks at $\boldsymbol{\theta_t = 40^\circ}$and around $\boldsymbol{95^\circ < \theta_t < 127^\circ}$ for Li+TF→LiF+T reaction. However, the absolute value of the different peaks for the Li+TF→LiF+T reaction is larger than that of Li+DF→LiF+D reaction at the same collision energy. These features reveal that the rotational alignment of the DF/TF products are not only along the $\mathbf{x+z}$ direction, but also along the $\mathbf{x-z}$ direction, and the degrees of rotational alignment of the TF product are stronger than that of DF product. In short, the isotopic substitution affects both the degree of rotational alignment and the direction of

product. Similar to $PDDCS_{21-}$, $PDDCS_{22+}$ is related to $\langle \sin^2\theta_r \cos 2\phi_r \rangle$ and the positive or negative values of $PDDCS_{22+}$ correspond to the product rotational alignment along the x-axis or y-axis. As shown in Figure 3.3 (b) and (d), $PDDCS_{22+}$ values vary with the change of scattering angle for each reaction, demonstrating that the DF/TF products angular momentum distribution are anisotropic. Furthermore, values of $PDDCS_{22+}$ are negative for each reaction, which indicates that the products rotational angular momentums are inclined to align along *y*-axis. In addition, the negative peaks appear around $\theta_t = 35^\circ$ and $\theta_t = 145^\circ$ for Li+DF→LiF+D reaction while the negative peaks appear around $\theta_t = 35^\circ$, $\theta_t = 90^\circ$ and $\theta_t = 140^\circ$ for Li+TF→LiF+T reaction. However, the absolute values of the different peaks for Li+TF→LiF+T reaction is less than that of Li+DF→LiF+D reaction at the same collision energy. These results are in good agreement with $P(\theta_r)$ distributions shown in Figure 3.1.

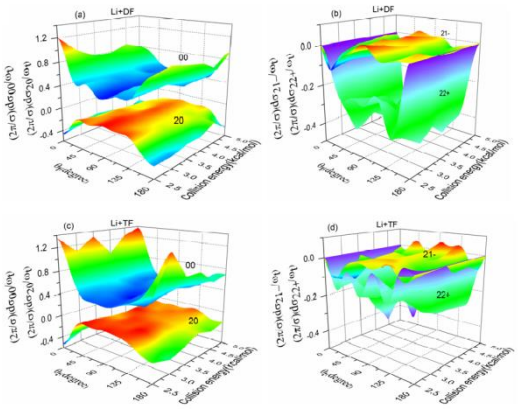

Figure 3.3: PDDCSs (a) $(2\pi/\sigma)(d\sigma_{00}/dw_t)(2\pi/\sigma)(d\sigma_{20}/dw_t)$ and (b) $(2\pi/\sigma)(d\sigma_{21-}/dw_t)(2\pi/\sigma)(d\sigma_{22+}/dw_t)$ for Li+DF→LiF+D reaction; (c) $(2\pi/\sigma)(d\sigma_{00}/dw_t)(2\pi/\sigma)(d\sigma_{20}/dw_t)$ and (d) $(2\pi/\sigma)(d\sigma_{21-}/dw_t)(2\pi/\sigma)(d\sigma_{22+}/dw_t)$ for Li+TF→LiF+T reaction at different collision energies.

4. Conclusions

In summary, the QCT method has been employed to investigate the stereodynamics for the title reactions at different collision energies based on the new PES constructed by Aguado *et al*. We calculated and discussed distributions of $P(\theta_r)$, $P(\phi_r)$, $\langle P_2(\cos\theta_r)\rangle$ and the four PDDCSs. The $P(\theta_r)$ distributions demonstrate a symmetric behavior about $\theta_t = 90^\circ$ for the title reactions, which displays that the product rotational angular momentum vector j' is strongly aligned along the direction perpendicular to the reagent relative velocity K for each reaction. Furthermore, the c of $P(\theta_r)$ distributions at $\theta_t = 90^\circ$ becomes weaker with the increment of the isotope mass. This conclusion can be confirmed by the computed values of the product rotational alignment parameters $\langle P_2(\cos\theta_r)\rangle$. The $P(\phi_r)$ distributions exhibit a large peak at $\phi_r = 270^\circ$ and no peak at $\phi_r = 270^\circ$ for all the reactions, which indicates that the product rotational angular momentum is oriented along the negative y-axis for Li+DF→LiF+D and Li+TF→LiF+T reactions. The $PDDCS_{00}$ distributions show forward and backward scattering for Li+DF/TF→LiF+D/T reactions. The $PDDCS_{20}$ distributions demonstrate an opposite trend to that of $PDDCS_{00}$. Moreover, $PDDCS_{20}$ is related to alignment moment $\langle P_2(\cos\theta_r)\rangle$. The $PDDCS_{21-}$ and $PDDCS_{22+}$ are equal to zero at the ends of forward and backward scatterings. Furthermore, The $PDDCS_{21-}$ and $PDDCS_{22+}$ distributions demonstrate that the product angular distributions are anisotropic.

Acknowledgements

This work was supported by National Natural Science Foundation of China (Grant No 11274205). The authors also appreciate Professor Keli Han for providing the QCT code of stereodynamics.

References

[1] C. H. Becker, P. Casavecchia, P. W. Tiedemann, J. J. Valentini, and Y. T. Lee, J. Chem.Phys, 73 (1980) 2833
[2] H. Loesch, E. Stenzel, and B. Wüstenbecker, J. Chem.Phys, 95 (1991) 3841
[3] H. J. Loesch and F. Stienkemeier, J. Chem.Phys, 99 (1993) 9598
[4] H. J. Loesch and F. Stienkemeier, J. Chem.Phys, 98 (1993) 9570
[5] O. Höbel, R. Bobbenkamp, A. Paladini, A. Russo, and H. J. Loesch, Phys. Chem. Chem. Phys., 6 (2004) 2198
[6] F. J. Aoiz, M. T. Martínez, and V. Sáez Rábanos, J. Chem.Phys, 114 (2001) 8880
[7] F. J. Aoiz, M. T. Martínez, M. Menéndez, V. Sáez Rábanos, and E. Verdasco, Chem. Phys. Lett, 299 (1999) 25
[8] P. F. Weck and N. Balakrishnan, J. Chem.Phys, 122 (2005) 154309
[9] M. Lara, A. Aguado, O. Roncero, and M. Paniagua, J. Chem.Phys, 109 (1998) 9391
[10] M. Lara, A. Aguado, M. Paniagua, and O. Roncero, J. Chem.Phys, 113 (2000) 1781
[11] M. Baer, I. Last, and H. J. Loesch, J. Chem.Phys, 101 (1994) 9648
[12] F. Gögtas, G. G. Balint-Kurti, and A. R. Offer, J. Chem.Phys, 104 (1996) 7927
[13] A. Lagana, A. Bolloni, S. Crocchianti, and G. A. Parker, J. Phys. Chem. A, 324 (2000) 466
[14] A. Aguado, M. Paniagua, M. Lara, and O. Roncero, J. Chem.Phys, 106 (1997) 1013
[15] G. A. Parker, A. Lagana, S. Crocchianti , and R. T. Pack, J. Chem.Phys, 102 (1995) 1238
[16] A. Aguado, M. Paniagua, M. Lara, and O. Roncero, J. Chem.Phys, 107 (1997) 10085
[17] A. Aguado, M. Paniagua, C. Sanz, and O. Roncero, J. Chem.Phys, 119 (2003) 10088
[18] A. Aguado, C. Sufirez, and M. Paniagua, Chem. Phys, 201 (1995) 107
[19] A. J. Hudson, H. B. Oh, J. C. Polanyi, and P. Piecuch, J. Chem.Phys, 113 (2000) 9897
[20] A.Lagana, A .Bolloni, and S. Crocchianti, Phys. Chem. Chem. Phys, 2 (2000) 535
[21] M. H. Yuan and G. J. Zhao, Int. J. Quantum Chem, 110 (2010) 1842
[22] R. S. Tan, X. G. Liu, and M. Hu, Chin. Phys. Lett, 29 (2012) 123101
[23] W. T. Li, M. D. Chen, and Z. G. Sun, J. Chem. Phys, 28 (2015) 415
[24] K. L. Han, G. Z. He, and N. Q. Lou, J. Chem.Phys, 105 (1996) 8699
[25] T. S. Chu, Y. Zhang, and K. L. Han, Int. Rev. Phys. Chem., 25 (2006) 201
[26] F. Aoiz, M. Brouard, V. Herrero, V. S. Rábanos, and K. Stark, Chem. Phys. Lett, 264 (1997) 487
[27] M. Wang, J. Chem. Phys., 109 (1998) 5446

[28] M. D. Chen, K. L. Han, and N. Q. Lou, J. Chem.Phys, 118 (2003) 4463
[29] M. L. Wang, K. L. Han , and G. Z. He, J. Phys. Chem. A,102 (1998) 10204
[30] Y. J. Wang , X. G. Liu , H. Z. Li, Q. Li, J. W. Chen, and Q. G. zhang, J. At. Mol. Sci, 6 (2015) 236
[31] M. L.Wang, K. L. Han, and a. G. Z. He, J. Chem.Phys, 109 (1998) 13
[32] X. G. Liu, H. Kong, W. W. Xu, J. J. Liang, F. J. Zong, and Q. G. Zhang, J. Mol. Struct. Theochem., 908 (2009) 117
[33] S. Y. Lin, K. L. Han, and J. Z. Zhang, Chem. Phys. Lett, 324 (2000) 122
[34] R. J. Li, K. L. Han, F. E. Li, R. C. Lu, G. Z. He, and N. Q. Lou, Chem. Phys. Lett, 220 (1994) 281
[35] T. S. Chu, H. Zhang, S. Yuan, A. Fu, H. Si, F. Tian, and Y. Duan, J. Phys. Chem. A, 113 (2009) 3470